Research Article

Preparation and Characterization of Double Shell Fe_3O_4 Cluster@Nonporous SiO_2@Mesoporous SiO_2 Nanocomposite Spheres and Investigation of their *In Vitro* Biocompatibility

Forough Toubi [1,2], Abdolkhalegh Deezagi [1], Gurvinder Singh [3], Mohammad Ali Oghabian [4], Seyed Safa Ali Fatemi [1], Ayyoob Arpanaei [1,*]

[1]Department of Industrial and Environmental Biotechnology, National Institute of Genetic Engineering and Biotechnology, Tehran, Iran
[2]Department of Chemical Engineering, Babol Noshirvani University of Technology, Babol, Iran
[3]Department of Materials Science and Engineering, Norwegian University of Science and Technology, Trondheim, Norway
[4]Research Center for Molecular and Cellular Imaging, Tehran University of Medical Science, Tehran, Iran

[*]*Corresponding Author*: Ayyoob Arpanaei, Department of Industrial and Environmental Biotechnology, National Institute of Genetic Engineering and Biotechnology, Tehran, Iran. Tel: +98-2144787463, E-mail: aa@nigeb.ac.ir

Received: December 07, 2014; **Revised:** January 23, 2015; **Accepted:** February 17, 2015

Background: Multifunctional core-shell magnetic nanocomposite particles with tunable characteristics have been paid much attention for biomedical applications in recent years. A rational design and suitable preparation method must be employed to be able to exploit attractive properties of magnetic nanocomposite particles.
Objectives: Herein, we report on a simple approach for the synthesis of magnetic mesoporous silica nanocomposite particles (MMSPs), consisted of a Fe_3O_4 cluster core, a nonporous silica shell and a second shell of the mesoporous silica of suitable sizes for biomedical applications and evaluate their cytotoxicity effects on human cancer prostate cell lines.
Materials and Methods: Clusters of magnetite (Fe_3O_4) nanoparticles were coated by a layer of nonporous silica using Stöber method. The coating step was completed by an outer layer of mesoporous silica via template-removing method. Structural properties of MMSPs were investigated by FTIR, HR-S(T)EM, BET, XRD techniques and magnetic properties of MMSPs by VSM instrument. MTT and LDH assays were employed to study the cytotoxicity of MMSPs.
Results: Obtained results revealed that decreasing the precursor concentration and the reaction time at the nonporous silica shell formation step decreases the thickness of the nonporous silica shell and consequently leads to the formation of smaller MMSPs. The as-prepared MMSPs have a desirable average size of 180±10 nm, an average pore size of 3.01 nm, a high surface area of 390.4 $m^2.g^{-1}$ and a large pore volume of 0.294 $cm^3.g^{-1}$. In addition, the MMSPs exhibited a superparamagnetic behavior and a high magnetization saturation value of 21±0.5 emu/g. Furthermore, the viability tests of DU-145 cell lines exposed to various concentrations of these particles demonstrated negligible cytotoxicity effects of the as-prepared particles.
Conclusions: These results demonstrate interesting properties of MMSPs prepared in this study for biomedical applications.

Keywords: Cytotoxicity; Nanocomposite magnetic particles; Silica shell

1. Background

In recent years, core-shell structured magnetic nanocomposite particles (NCPs) have extensively been produced and evaluated. The combined simultaneously functionalities of cores and shells of these materials can be exploited in different applications (1, 2). NCs have exhibited wonderful potentials in magnetically targeted carrier system for drug delivery, bioseparation, enzyme immobilization, diagnostics and analysis (3, 4). Iron oxide nanoparticles (magnetite or maghemite) with diameters less than 15 nm possess superparamagnetic properties (5), and can be used as a magnetic resonance imaging (MRI) contrast agent. A thin layer of a material like silica as a coating shell can protect magnetite nanoparticles from intersystem dipolar interactions, agglomerations, undesirable influences of the surrounding materials and improving the magnetic core stability under harsh conditions. However, the nonmagnetic silica shell causes the decrease of magnetization (6). A strategy to overcome this limitation is to form a core of iron oxide NPs clusters with strong magnetization. In such structures,

each NP is constituted by a magnetic core consisted of several magnetite NPs that maintain the superparamagnetic behavior of iron oxide nanoparticles and prepare a high volume magnetic moment together. Stabilizing magnetite NPs clusters is achieved through formation of a nonporous silica shell. The mesoporous silica shell makes MMSPs a superior candidate for drug delivery owing to its ease of surface functionalization, biocompatibility and biodegradability, extraordinary physicochemical stability and high surface area and pore volume where sufficient amount of drug can be loaded (7, 8).

In biological systems, sequestration by phagocytotic cells and the time of blood circulation of particles are affected by their size. It has been repeatedly emphasized that the surface characteristic and of NPs are of importance in terms of interaction with biological systems, clearance and toxicity. In contrast to crystalline silica, amorphous silica is highly biocompatible and nontoxic that causes no adverse tissue reactions (9). Amphiphilic properties of silica will extend the blood circulation time (10). In general, keeping the particle size between 50 to 300 nm enhances its hydrodynamic stability in the blood circulation (11). Significant proportion on NPs above 300 nm in diameter, are mechanically filtered in the lung. For instance, Brochardt and coworkers (1994) injected silica (SiO_2) particles with 600 nm diameter into rats. A day after injection, half the particles were found in lungs and 40% in liver (12). Particles smaller than 50 nm leave the blood vessels through extravasation and renal clearance and thus tend to distribute nonspecifically in body (13). He *et al*. (2008) investigated a mouse model for biodistribution of three types of surface-modified SiO_2 NPs doped with RuBPY with a diameter of 45 nm used for imaging purposes. All different types of injected silica NPs were rapidly (3 to 5 h) cleared from systemic blood circulation (14). SiO_2 elimination process was considered by Borak and coworkers (2012). They found that 36% of the SiO_2 (150 nm) particles are excreted with urine after 4 days and the remaining particles are accumulated in kidneys and lungs (15).

Toxicity of NPs on biological entities is also highly dependent to their size, shape, structural properties, dosage and cell types (16). Up to now, the biocompatibility of silica-coated magnetic nanoparticles has been investigated through various studies. Singh and coworkers (2012) created silica-coated magnetite NPs with sizes from 15 to 270 nm using the sol-gel method. *In vitro* assay by CCK-8 on MC3T3-E1 cells at different concentrations of NPs during 48 h of culture confirmed the negligible cytoxicity effect of NPs. They reported that the smaller particles less than 100 nm were more toxic affecting the exposed cells much more faster once compared with larger sizes (17). In another research, Zhang and co-workers (2010) studied the biocompatibility of 80 and 500 nm silica NPs on human dermal fibroblasts. They found that cell viability and mitochondrial membrane potential are most strongly affected by the smaller NPs in comparison to those of the larger NPs (18). The composites of maghemite NPs embedded in an ordered mesoporous silica matrix with a size of 0.3 to 3 μm were produced by Saavedra (2010) for hyperthermia therapy. The synthesized magnetic mesoporous silica spheres showed excellent biocompatibility when applied to cultures of A549, Saos-2 and HeLa-derived tumor cell lines using LDH release assay. Those results also indicated that fractions of particles having larger sizes do not reach the inner cells (19).

To the best of our knowledge, no reports are available on the synthesis of adjustable sized magnetic mesoporous silica particles consisting of a magnetic core of magnetite NP clusters. Accordingly, no in vitro biocompatible analysis is expected to be found in literature. However, synthesis of 450 nm MMSPs and a magnetic core diameter of about 75 nm has been reported earlier (20). Obviously, such large sizes are not suitable for drug delivery and bioimaging purposes. Due to the importance of size of magnetite silica NPs for biomedical applications, MMSPs with core/double shell and sizes between 100 to 300 nm were synthesized. MMSPs consisted of a magnetic cluster core, a thin layer of nonporous silica shell and outer mesoporous silica shell. The synthesis of such MMSPs will be achieved via controlling the size of nonporous silica shell. The cytotoxicity of such MMSPs was evaluated using DU-145 adhesive epithelial cells via MTT and LDH assays.

2. Materials and Methods

Ferric chloride hexahydrate ($FeCl_3.6H_2O$), ferrous chloride tetrahydrate ($FeCl_2.4H_2O$), ammonium hydroxide (28-30%), tetraethyl orthosilicate (TEOS) (99.9%), ethanol (99.9%), oleic acid, toluene, hexane, acetone and cetyltrimethylammonium bromide (CTAB) were all obtained from Merck (Germany). Dulbecco's modified eagle medium (DMEM), fetal bovine serum and penicillin/streptomycin was purchased from Gibco (Grand Island, USA). 3-[4,5-Dimethylthialzol-2-yl]-2,5-diphenyltetrazolium bro-

mide (MTT) was obtained from Sigma Chemical Company (St. Luis, MO, USA). LDH Kit was obtained from Ziestchem Diagnostics Company (Tehran, Iran). Deionized water (DI) with resistivity of higher than 18 MΩ was used in all experiments.

2.1. Synthesis of Fe_3O_4 Cluster@Nonporous SiO_2@Mesoporous SiO_2 (MMSPs)

2.1.1. Synthesis of Oleic Acid-Coated Fe_3O_4 NPs

The magnetite NPs were prepared by co-precipitation of Fe(II) and Fe(III) chlorides in an ammonia solution using a method previously described (21). The coating of oleic acid on magnetite NPs was planned to improve dispersible ability of magnetite NPs (22). Typically, to prepare magnetite NPs, a 60 mL solution of dissolved iron salts (199 mg of $FeCl_2.4H_2O$ and 540 mg of $FeCl_3.6H_2O$) in DI water was mechanically stirred at 1000 rpm under nitrogen gas. After 5 min, 0.1 mL of oleic acid was added to the salt solution and subsequently the precipitation was performed by addition of 7.5 mL of ammonium solution. The mixture was heated up to 80ºC and 0.4 mL oleic acid was added in 4 steps within 15 min to obtain the coating. The black precipitated oleic acid-coated magnetite NPs was cooled to room temperature and magnetically recovered. The product was washed 3 times with DI water to remove the excess by-products.

2.1.2. Synthesis of Core/shell Fe_3O_4 Cluster@Nonporous SiO_2 Particles (MSPs)

In this part, a thin nonporous silica shell surrounding the magnetite cluster NPs was formed based on Stöber method (23). To form Fe_3O_4 cluster cores, two methods developed by Taboada *et al*. (24) and Woo *et al*. (25), respectively with some modifications (20). Based on the first method typically, 20 mg of re-dispersed oleic acid-coated magnetite NPs in 2.4 mL hexane was added dropwise to 60 mL acetone under nitrogen gas and vigorous stirring at 1200 rpm, while the acetone/hexane volume ratio was 25. After 3 min of mixing, the speed of mixing reduced to 400 rpm and 3 mL of ammonia solution was added. After 1 min, 0.5 mL of TEOS was added to the reaction mixture dropwise in 15 min and the mixing was continued at 400 rpm at room temperature for 24 h to complete reaction. The resulting product (designated MSP1) was collected with a magnet and washed repeatedly with ethanol and DI water. Four other samples were prepared based on the second method (25) with some modifications. In brief, 75 mg of magnetite NPs were dispersed in 5 mL of toluene and mixed with a mixture of 80 mL of ethanol, 20 mL of DI water and 2.5 mL of ammonia solution, followed by mechanically stirring at 350 rpm and room temperature for 20 min. TEOS (0.5 or 1 mL) added dropwise to the solution within 30 min. After 4 h, the nonporous silica shell was formed and the obtained core/shell silica-coated magnetic particles (MSP2 and MSP3 samples prepared using 0.5 or 1 mL TEOS, respectively) were separated with a magnet and washed repeatedly with ethanol and DI water. MSP4 and MSP5 samples were prepared under the same condition unless an extended reaction time in the nonporous silica shell formation step (24 h instead of 4 h) was applied.

2.1.3. Coating MSPs with a Mesoporous Silica Shell

MSPs of desired size, shape and monodispersity were chosen for the formation of the mesoporous silica shell using the surfactant-template removing method (26) with some modifications as described before (27). Typically, 0.15 g of CTAB was dispersed in a mixture of 40 mL of DI water, 0.55 mL of ammonia solution and 30 mL of ethanol. MSPs (30 mg) were mixed with the prepared mixture and stirred mechanically at room temperature for 20 min. TEOS (0.21) was added and the reaction was allowed to proceed for 6 h. The resulting MMSPs were collected with magnet and washed several times with ethanol and DI water, dried at 80ºC and calcinated at 600ºC for 5 h to extract CTAB and produce mesoporous silica shell. The resulting MMSPs washed repeatedly with DI water.

2.2. Cell Culture

The human prostate cancer cell lines DU-145 were routinely cultured in DMEM supplemented with 10% (v/v) fetal bovine serum and 120 $mg.L^{-1}$ penicillin and 220 $mg.L^{-1}$ streptomycin at 37ºC in a humidified 5% CO_2 atmosphere.

2.3. Characterization of the As-Prepared Particles

The morphology of as-prepared particles was investigated using HR-S(T)EM with a Philips CM 200 microscope operated at an accelerating voltage of 200 kV. The particle size, size distribution and zeta potential of nanoparticles in solution was measured with Zetasizer Nano ZS apparatus (Malvern, UK). The X-ray diffraction (XRD) analysis was performed with a Bruker D8 advance x-ray diffractometer (Bruker, Germany). The porous structure of as-prepared MMSPs was characterized using nitrogen/sorption isotherms. The pore characteristics of MMSP was measured according to the BET and BJH method from

the adsorption branches of the isotherms obtained in 77 K on Belsorp mini II analyzer. The magnetic properties of as-prepared particles were analyzed under a varying magnetic field using a vibration sample magnetometer (VSM, Meghnatis Daghigh Kavir Co., Iran).

2.4. In vitro Cytotoxicity Assays

2.4.1. MTT Assay for Cellular Viability

The cell viability of selected NCPs was evaluated using MTT assay. This assay is based on a colorimetric assay in which the dark blue formazan crystals are formed from splitting of tetrazolium rings of the pallid yellow MTT due to activity of a mitochondrial dehydrogenase enzyme from viable cells (28). In this assay briefly, 2×10^4 cells were seeded in each well of a 96-well flat-bottom plate and were incubated at 37ºC and 5% CO_2 for 24 h. MMSPs in PBS (10 µL of 1, 10, 40, 100 and 200 $\mu g.L^{-1}$) were added to cells and incubated as above for 24 h. MTT (10 µL of 5 $mg.L^{-1}$) reagent was added to each well and the plate incubated for 4 h at 37ºC to allow formazan dye to form. The culture medium of each well was discarded and dimethyl sulfoxide (DMSO) (100 µL) was added to dissolve dark blue formazan crystals for 15 min. The absorbance was monitored using an ELISA microplate reader (Labsystem multiscan, Ontario, Canada) at 580 nm. The experiments were repeated 3 times under the same condition.

2.4.2. Lactate Dehydrogenaze (LDH) Assay

LDH assay is a trustworthy colorimetric assay, which determines LDH activity in the culture medium as a marker for cytotoxicity using a commercial LDH Kit according to the instructions. Released LDH catalyzed the reduction of NAD^+ to NADH, so the rate of NAD^+ reduction was clearly proportional to LDH activity in the cell medium. After exposure to different concentrations of MMSPs (1, 10, 40, 100 and 200 $\mu g.L^{-1}$) for 24 h, 1000 µL of cell media was used for the LDH assay. The absorbance was measured by using the UV-Vis spectrophotometer T80 (PG instruments Ltd, England) at 340 nm. The experiments were repeated 3 times under the same condition.

3. Results

3.1. Synthesis of Magnetite Cluster/Nonporous Silica/Mesoporous Silica Core/Double Shell NCs

TEM image of oleic acid-coated magnetite NPs indicated that the 7.5 nm as-prepared NPs were uniform in size (Figure 1A). X-ray diffraction (XRD) patterns were analyzed to determine crystal phase of NPs.

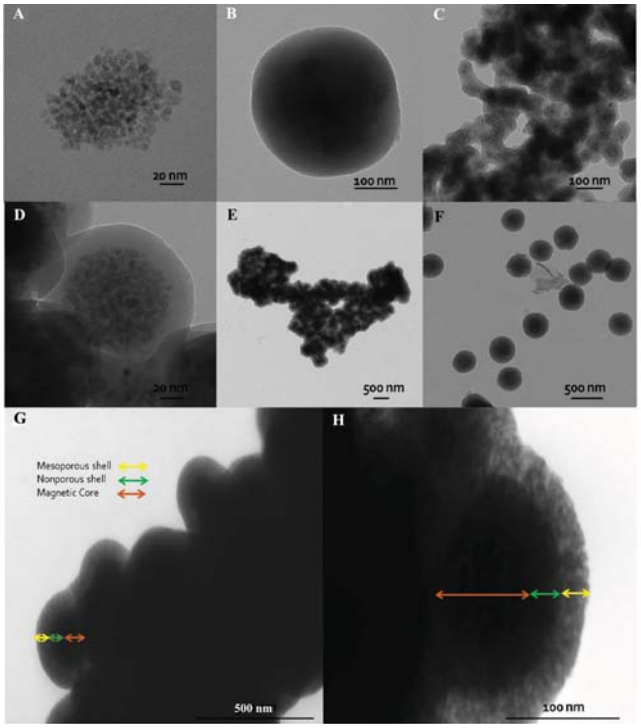

Figure 1. Transmission electron microscopic images of A: magnetite, B: MSP1, C: MSP2, D: MSP3, E: MSP4, F: MSP5, G,H: MMSP3

Magnetite NPs showed diffraction peaks at 2θ ~30°, 35.5°, 43°, 53.5°, 57° and 62.5°, which are characteristic peaks of magnetite crystal structure (29). These characteristic diffraction peaks indicated by their indices, (220), (311), (400), (511) and (440), that have been well indexed to the inverse spinel structure of Fe_3O_4 (Joint Committee on Powder Diffraction Standards card no. 85-1436; Figure 2A). The silica shell was formed on magnetite cluster via two methods. According to TEM images, the average size of MSPs produced by acetone/hexane solution is estimated to be about 320±10 nm that is not useful for our applications (Figures 1B). Figures 1C-F represent TEM images of Fe_3O_4 cluster@nonporous silica particles produced by toluene in different reaction conditions (Table 1). The NPs size in solution was determined by the DLS measurements and confirmed TEM results (Table 1). Figure 2B shows XRD pattern of magnetite cluster/nonporous silica core/shell MSP3 NPs. The XRD pattern was similar to that of the magnetite NPs. A little reduction in peaks' intensity however; was due to the amorphous structure of silica shell. According to the characteristic peak at around 2θ =20°, the formation of the silica coating around mag-

Table 1. Conditions employed in the synthesis of various samples and the properties of the as-prepared samples

Sample	Clustering solution	TEOS Conc.1 (mol.L^{-1})	T_1 (h)	TEOS Conc.2 (mol.L^{-1})	T_2 (h)	NP size (nm) (TEM)	NP size (nm) (DLS)	Saturation magnetization (emu.g^{-1})
MSP1	Acetone	3.41×10^{-2}	24	-	-	320±10	330±10	24±1
MSP2	Toluene	2.06×10^{-2}	4	-	-	110±10	125±10	-
MSP3	Toluene	4.12×10^{-2}	4	-	-	148±10	160±10	-
MSP4	Toluene	2.06×10^{-2}	24	-	-	180±10	190±10	-
MSP5	Toluene	4.12×10^{-2}	24	-	-	400±10	415±10	-
MMSP1	Acetone	3.41×10^{-2}	24	1.32×10^{-2}	6	450±10	460±10	9±1
MMSP2	Toluene	2.06×10^{-2}	4	1.32×10^{-2}	6	130±10	140±10	24±1
MMSP3	Toluene	4.12×10^{-2}	4	1.32×10^{-2}	6	180±10	200±10	21±1
MMSP4	Toluene	2.06×10^{-2}	24	1.32×10^{-2}	6	240±10	250±10	14±1
MMSP5	Toluene	4.12×10^{-2}	24	1.32×10^{-2}	6	480±10	500±10	12±1

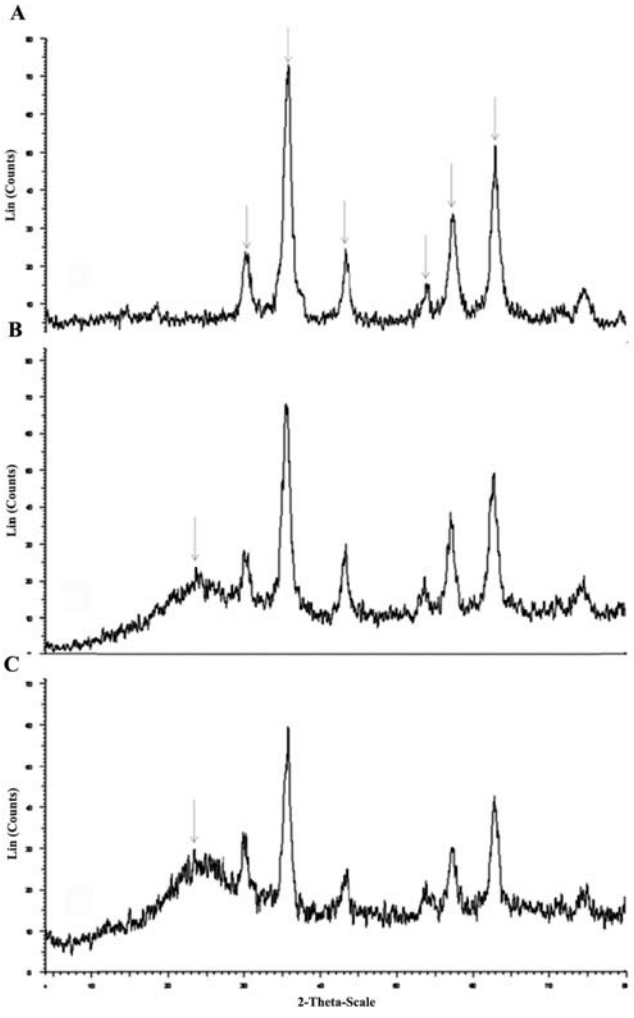

Figure 2. The X-ray diffraction patterns of A: magnetite NPs, B: MSP3 and C: MMSP3

netite cluster core is confirmed (30). These results revealed that, the existence of silica shell layer on the surface of Fe_3O_4 nanoparticles does not lead to their crystal phase change. TEM images revealed that the diameter of magnetite cluster core in NPs synthesized by toluene is about 75±10 nm. The concentration of TEOS was found to have a significant influence on the thickness of the silica shell. The thickness of silica shell was increased with increasing the concentration of TEOS (Table 1). Finally, a shell of mesoporous silica formed on MSPs by surfactant template removing. Fourier transform IR (FT-IR) results indicated that CTAB is completely removed via this procedure as the IR absorption at 1400-1600^{-1} and 2800-3000^{-1}, which are characteristic peaks of CTAB molecules, were absent in the FT-IR spectra of surfactant-extracted MMSPs (Figure 3). As TEM images show the as-prepared MMSP3 particles had spherical shapes with an average size of 180 nm (Figures 1G, H) and district nonporous and mesoporous shells with a thickness of 25 and 30 nm, respectively were noted. While, the

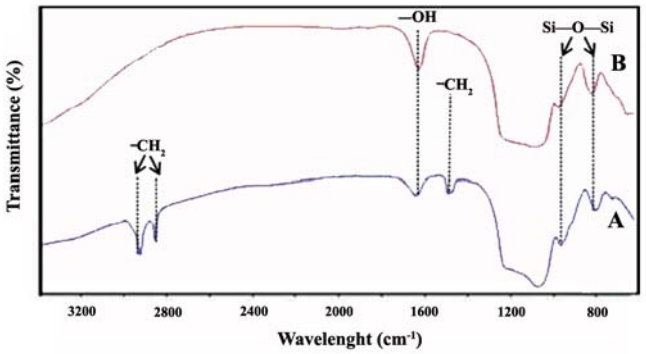

Figure 3. FT-IR of MMSP3 A: before calcination, B: after calcination

DLS average size of these particles was measured to be 190 nm (Table 1). The measured zeta potential of MMSPs was -30.4 mV. The negative charge of synthesized MMSPs can be attributed to -OH groups existing on the surface of particles.

The characteristic peaks of MMSP3 in XRD pattern at 2θ =23° are compatible with standard peaks of silica (Figure 2C). A single reflection with intensity maximum in low-angle XRD pattern indicated that the mesoporous structure nature exists on MMSP3. After extraction of CTAB molecules, the mesoporous silica shell of MMSP3 provided high surface area and pore volume values, measured by the N_2 adsorption/desorption isotherms (Figure 4). The corresponded Barrett-Joyner-Halenda (BJH) pore size characterized to be 2.42 nm. The (BET) surface area, total pore volume and mean diameter pore were calculated to be 390.4 $m^2.g^{-1}$, 0.2939 $m^3.g^{-1}$ and 3.011 nm, respectively.

The vibrating-sample magnetometer (VSM) was used to investigate the magnetic properties of all samples (magnetite NPs, MSP3 and MMSP3). Magnetic characterization indicated that the magnetite NPs, MSP3 NPs and MMSP3 NCPs have magnetization saturation values of 60±0.5, 24±0.5 and 21±0.5 emu/g, respectively (Figure 5).

3.2. Analysis of In Vitro Cytotoxicity of MMSP3s

We employed the standard MTT and LDH assays using various MMSPs concentrations (1-200 $\mu g.mL^{-1}$) to examine the *in vitro* cytotoxicity of the as-prepared particles. Figure 6 shows the viability profile of the DU-145 adhesive epithelial cells treated with the as-prepared MMSPs after 24 h incubation. It can be seen that MMSPs present statistically negligible cytotoxicity effects; even at high concentrations such as 200 $\mu g.mL^{-1}$ with 93% cell viability. The results of LDH leakage assay were consistent with the MTT viability results. The amount of released LDH is proportional to the number of cells damaged or lysed and is a useful index for assessment of cytotoxicity based on the loss of membrane integrity. LDH levels were increased in a dose-dependent manner (Figure 7), but the alterations were not significant once compared with the control. The MTT and LDH assays do not follow any specific patterns between increasing the NCPs concentration and cell viability and LDH release. However, both were in close agreement with results previously reported elsewhere (17, 18), implying synthesized NCPs to be biocompatible.

4. Discussion

4.1. NPs Synthesize

Magnetite NPs coated with oleic-acid were produced by co-precipitation approach in which Fe (II) and Fe (III) salts were reduced by ammonium solution in the presence of nitrogen atmosphere to avoid oxida-

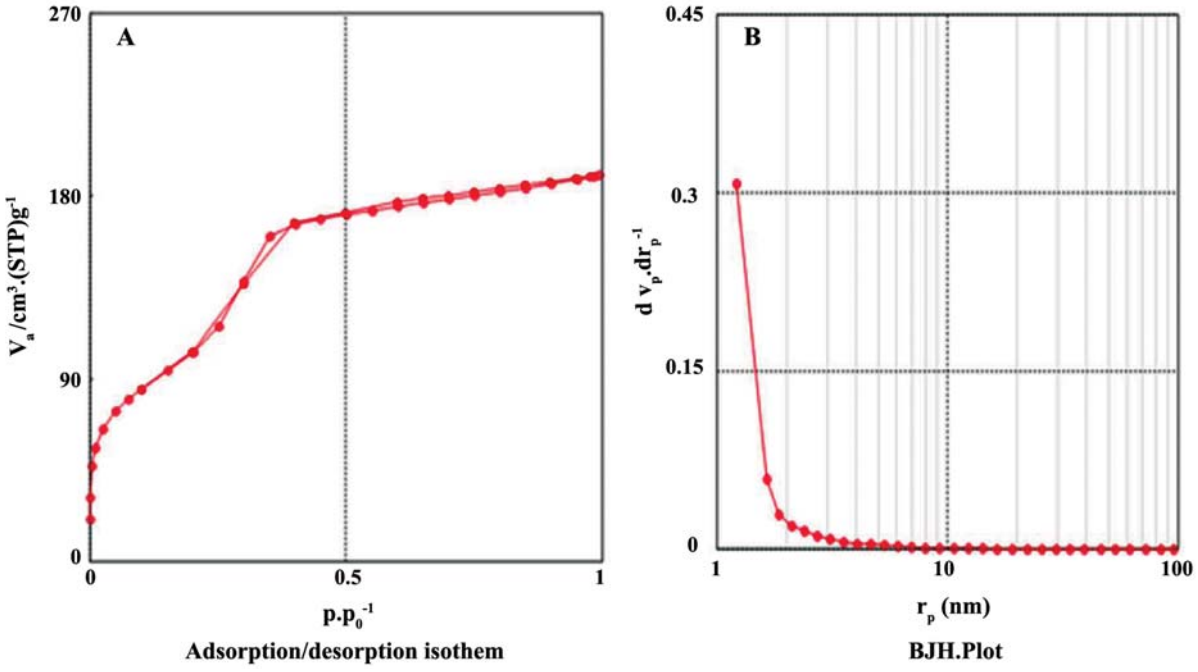

Figure 4. A: Nitrogen adsorption-desorption isotherms, B: the BJH plot of MMSP3

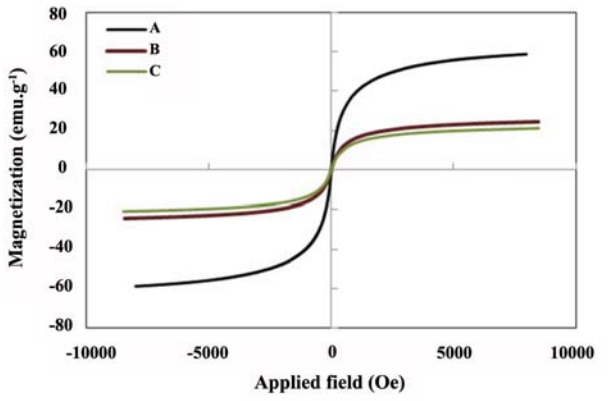

Figure 5. Magnetic hysteresis loops of A: magnetite, B: MSP3, C: MMSP3 at room temperature

tion (Figure 1A). Magnetite NPs synthesized by this method normally have an undesired characteristic, *i.e.* they tend to agglomerate that could apparently be due to magnetic dipole-dipole interactions, the Van der Waals force between magnetic NPs and reduction of surface energy of magnetic NPs. Magnetite NPs agglomeration leads to substantial specific surface area built-up (31). The surface coating of magnetic NPs with oleic acid would be expected to prevent magnetic NPs aggregation by electrostatic repulsion between the negatively-charged surface carboxylate groups (32). To obtain core/shell NPs with a core of magnetite cluster surrounded by a thin nonporous silica shell, we used two procedures for synthesis of magnetite cluster cores. The Stöber method was employed to make the nonporous silica shell (23). The Stöber method is based on mixing TEOS as the silica precursor in a water-alcohol solution in the presence of ammonia to make an alkaline condition that helps to accelerate polymerization of TEOS to form the silica shell. In the first method, the acetone/hexane solution with the volume ratio of 25 was used to form the magnetite NPs core (25). The oleic acid-coated magnetite NPs are stable in hexane and unstable in acetone, so they tend to self-assemble into clusters in a mixture of these solvents. The as-prepared magnetite clusters served as the nucleation site for condensation of hydrolyzed TEOS and construction of the silica shell (Figure 1B). Furthermore, oleic acid-coated magnetite NPs were re-dispersed in toluene, forming emulsion drops by the addition of ethanol. The same as previous method, the silica shell was formed via the hydrolysis and condensation of TEOS around the magnetite cluster cores (Figure 1C-F).

The discrepancy between the NPs diameter of samples that produced by toluene solution might be explained by varying the concentration of TEOS, that is added into the reaction mixture simultaneously during the clustering of the magnetite NPs. Additionally, NPs diameters were under the influence of reaction time. A surface reaction-limited condensation of hydrolyzed monomers enhances the growth. Aggregation process of siloxane substructures led particle formation. Ionic strength of the reaction medium and particles size had influence on the particle formation. Thus, stability of the silica NPs in alcohol, water and ammonia mixture had a major role in its size. Moreover, NPs size is dependent on the constant rates of hydrolysis and condensation steps as a function of the reaction mixture (33). Similar to earlier works (17, 34-35), we demonstrated that silica shell thickness around magnetite nanoparticles will increase with

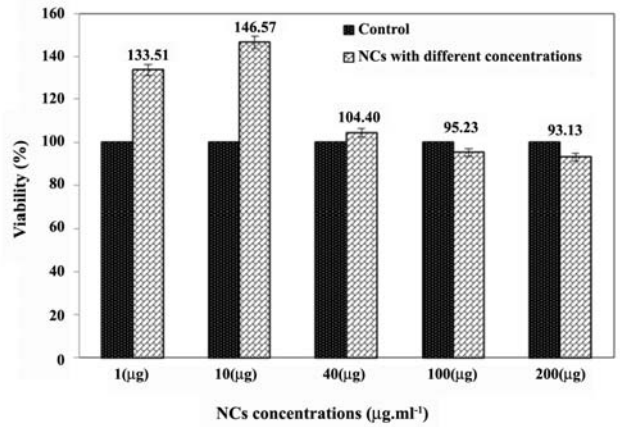

Figure 6. *In vitro* viability DU-145 cells treated with different concentration of MMSP

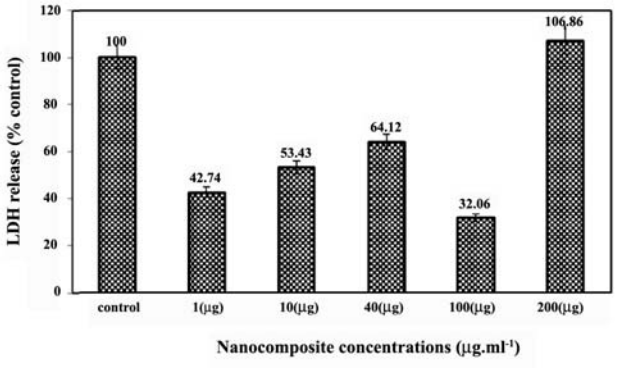

Figure 7. LDH assay of DU-145 cells in the presence of different concentration of MMSP3

increasing the TEOS amount and the size of silica NPs. The latter itself is being increased by increasing the concentration of the precursor. Moreover, reduction in synthesis time (from 24 to 4 h) caused a reduction in nonporous silica shell thickness in the same reactant concentration. It has been reported that a thicker silica shell is obtained when the reaction time and TEOS concentration are increased (36). Therefore, smaller silica-coated magnetic particles are obtained at 4 h reaction time and TEOS concentration of 4.12×10^{-2} $mol.L^{-1}$ were employed (Table 1).

In the next step, MS particles were used to be covered by a thin shell of the mesoporous silica shell. CTAB was used as the surfactant-template to form the mesoporous structure. The surfactant template molecules were extracted by calcination method (26). The dispersion stability of synthesized MMSP in aqueous solution remained stable for several days (Figure 8).

According to the N_2 adsorption-desorption isotherms, the curve of adsorption isotherm sharply increased at low relative pressure and gradually increased to a maximum relative pressure (Figure 4A). The curve shows the typical type IV isotherm according to IUPAC classification, characterizing the mesoporous structures. The average pore size of nanocomposite was determined by the BET method. The BET plot of pore diameters showed an average pore size of 3.01 nm for the synthesized magnetic particles.

The lower magnetic saturation value for MSP and MMSP nanocomposites could be explained by the presence of non-magnetic layer of mono shell of nonporous silica and double shell of nonporous and mesoporous silica around magnetic core of the two samples (Figure 1G and 1H). These layers weaken the magnetic moment of the inner core of magnetite clusters, as reported earlier (34). Clearly, no remanence of NPs demonstrated that all samples are superparamagnetic. The MMSPs were dispersed in a water and ethanol solution without any flocculation (Figure 8A). As soon as they placed near to external magnetic field, they moved to the side of the vial (Figure 8B). These observations imply the as-prepared nanocomposite magnetic particles possess excellent superparamagnetic properties, which is a compulsory property for potential biomedical applications.

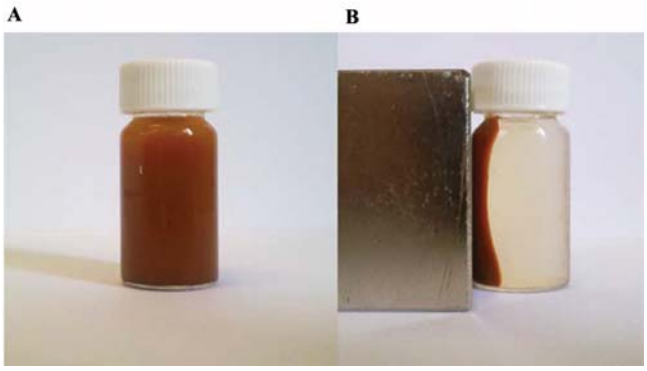

Figure 8. The as-synthesized MMSP3 dissolved in water: A: well dispersed without the presence of external magnetic field, B: collected to the wall of sample vial upon the placement of a magnet

4.2. In Vitro Biocompatibility Assays

The prepared MMSPs should be investigated for their biocompatibility in order to envisaged in biomedical applications. It is documented that amorphous silica NPs are reasonably non-toxic and biocompatible, but the surfactant CTAB is renowned as a cytotoxic material (37). Here, CTAB molecules were extracted and completely removed once MMSPs were prepared. As a result, the surfactant-extracted MMSPs are expected to be non-cytotoxic and our data were suggestive great biocompatibility and relatively low cytotoxicity (Figures 6 and 7). These results are in agreement with those obtained by Huang *et al*. (38) which showed the suitable viability of fibroblast cells incubated over a wide range of dosages (1.5 to 100 $\mu g.mL^{-1}$) of magnetic mesoporous silica nanocomposite particles. They reported small negligible differences in cell viability after 24 h of incubation and a slight cytotoxicity at a high concentration (100 $\mu g.mL^{-1}$) of NCs. However, we believe that it is essential to explore novel approved tools and carry out more in-depth studies to elucidate cellular response mechanism to NCs.

5. Conclusions

We prepared MMSPs of desired average sizes (about 180 nm), consisting of a magnetite cluster core encapsulated in the double nonporous-mesoporous silica shell with a high surface area and narrow pore size. The developed synthetic protocol can be generalized to produce the MMSPs with different sizes by varying the thickness of the inner nonporous silica shell for various applications. The as-prepared MMSPs combine the excellence of both magnetic core and mesoporous silica shell. Our results demonstrated that the MMSPs possess a suitable superparamagnetic property and low toxicity, which are essential properties for biomedical applications.

Acknowledgements

The authors would like to thank Iran National Science Foundation (INFS) for the financial support.

References

1. Chan Y, Zimmer JP, Stroh M, Steckel JS, Jain RK, Bawendi MG. Incorporation of Luminescent Nanocrystals into Monodisperse Core-Shell Silica Microspheres. *Adv Mater*. 2004;**16**(23-24):2092-2097. DOI: 10.1002/adma.200400237
2. Deng YH, Yang WL, Wang CC, Fu, SK. A novel approach for preparation of thermal responsive polymer magnetic microsphere with core-shell structure. *Adv Mater*. 2003;**15**(20):1729-1732. DOI: 10.1002/adma.200305459
3. Nitin N, Laconte LEW, Zurkiya O, Hu X, Bao G. Functionalization and peptide-based delivery of magnetic nanoparticles as an intracellular MRI contrast agent. *J Biol Inorg Chem.* 2004;**9**(6):706-712. DOI: 10.1007/s00775-004-0560-1
4. Lee DG, Ponvel KM, Kim M, Hwang S, Ahn IS, Lee CH. Immobilization of lipase on hydrophobic nano-sized magnetite particles. *J Mol Catal B Enzym.* 2009;**57**(1-4):62-66. DOI: 10.1016/j.molcatb.2008.06.017
5. Namdeo M, Saxena S, Tankhiwale R, Bajpai M, Mohan YM, Bajpai SK. Magnetic nanoparticles for drug delivery applications. *J Nanosci Nanotechnol*. 2008;**8**(7):3247-3271. PMID: 19051873
6. Kim HJ, Kwon HS, Ahn JO, Lee CH, Ahn IS. Evaluation of a silica-coated magnetic nanoparticle for the immobilization of a His-tagged. *Biocatal Biotransform*. 2009;**27**(4):246-253. DOI: 10.1080/10242420903042627
7. Vallet-Regi M, Balas F, Arcos D. Mesoporous materials for drug delivery. *Angew Chem Int Ed*. 2007;**46**(40):7548-7558. PMID: 17854012
8. Slowing II, Trewyn BG, Lin VSY. Mesoporous silica nanoparticles for intracellular delivery of membrane-impermeable proteins. *J Am Chem Soc*. 2007;**129**(28):8845-8849. DOI: 10.1021/ja0719780
9. Liu HM and Hsiao JK. *Magnetic Nanoparticles: Its Effect on Cellular Behaviour and Potential Applications, Smart Nanoparticles Technology*. Dr. Abbass Hashim (Ed.). 2012;P. 357-376. ISBN: 978-953-51-0500-8, In Tech. DOI: 10.5772/34252
10. Kortesuo P, Ahola M, Karlsson S, Kangasniemi I, Yli-Urpo A, Kiesvaara J. Silica xerogels as an implantable carrier for controlled drug delivery-evaluation of drug distribution and tissue effects after implantation. *Biomat*. 2000;**21**:193-198. DOI: 10.1016/S0142-9612(99)00148-9
11. Jain RK. Delivery of molecular and cellular medicine to solid tumors. *Adv Drug Deliv Rev.* 2001;**46**(1-3):149-168. PMID: 11259838
12. Borchardt G, Brandriss S, Kreuter J, Margel S. Body distribution of 75Se-radiolabeled silica nanoparticles covalently coated with omega-functionalized surfactants after intravenous injection in rats. *J Drug Targ.* 1994;**2**(1):61-77. PMID: 8069585
13. Gupta AK, Gupta M. Synthesis and surface engineering of iron oxide nanoparticles for biomedical applications. *Biomat.* 2005;**26**(18);3995-4021. PMID: 15626447
14. He X, Nie H, Wang K, Tan W, Wu X, Hang P. *In vivo* study of biodistribution and urinary excretion of surface-modified silica nanoparticles. *Anal Chem.* 2008;**80**(24):9597-9603. DOI: 10.1021/ac801882g
15. Borak B, Biernat P, Prescha A, Baszczuk A, Pluta J. In VivoStudy on the Biodistribution of Silica Particles in the Bodies of Rats. *Adv Clin Exp Med*. 2012;**21**(1):13-18. PMID: 23214294
16. Kong B, Seog JH. Graham LM, Lee SB. Experimental considerations on the cytotoxicity of nanoparticles. *Nanomed* (Lond). 2011;**6**(5):929-941. DOI: 10.2217/nnm.11.77
17. Singh RK, Kim TH, Patel KD, Knowles JC, Kim HW. Biocompatible Magnetite Nanoparticles with Varying Silica Coating Layer for Use in Biomedicine; Physicochemical and Magnetic Properties and Cellular Compatibility. *J Biomed Mater Res A*. 2012;**100**(7):1734?1742. DOI: 10.1002/jbm.a. 34140
18. Zhang Y, Hu L, Yu D, Gao C. Influence of silica particles internalization on adhesion and migration of human dermal fibroblasts. *Biomaterials*. 2010;**31**(32):8465-8474. DOI: 10.1016/j.biomaterials.2010.07.060
19. Martín-Saavedra FM, Ruíz-Hernández E, Boré A, Arcos D, Vallet-Regí M, Vilaboa N. Magnetic mesoporous silica spheres for hyperthermia therapy. *Acta Biomater.* 2010;**6**(12):4522-4531. DOI: 10.1016/j.actbio.2010.06.030
20. Kalantari M, Kazemeini M, Tabandeh F, Arpanaei A. Lipase immobilisation on magnetic silica nanocomposite particles: effects of the silica structure on properties of the immobilised enzyme. *J Mater Chem*. 2012;**22**:8385-8393. DOI: 10.1039/C2JM30513E
21. Silva RN, Asquieri ER, Fernandes KF. Immobilization of Aspergillus niger glucoamylase onto a polyaniline polymer. *Process Biochem.* 2005;**40**(3-4):1155-1159. DOI: 10.1016/j.procbio.2004.04.006
22. Prakash A, Zhu H, Jones CJ, Benoit DN, Ellsworth AZ, Colvin VL. Bilayers as phase transfer agents for nanocrystals prepared in nonpolar solvents. *ACS Nano*. 2009;**3**(8):2139-2146. DOI: 10.1021/nn900373b
23. Stöber W, Fink A, Bohn E. Controlled growth of monodisperse silica spheres in the micron size range. *J of Coll and Int Sci.* 1968;**26**(1):62-69. DOI: 10.1016/0021-9797(68)90272-5
24. Taboada BE, Solanas R, Rodriguez E, Weissleder R, Roig A. Supercritical-Fluid-Assisted One-Pot Synthesis of Biocompatible Core(γ-Fe_2O_3)/Shell(SiO_2) Nanoparticles as High Relaxivity T_2-Contrast Agents for Magnetic Resonance Imaging. *Adv Func Mater.* 2009;**19**(14):2319-2324. DOI: 10.1002/adfm.200801681
25. Chen DH, He XR. Synthesis of nickel ferrite nanoparticles by sol-gel method. *Mater Res Bull*. 2001;**36**(7-8):1369-1377. DOI: 10.1016/S0025-5408(01)00620-1
26. Hu C, Gao Z, Yang X. Fabrication and magnetic properties of Fe_3O_4 octahedra. *Chem Phys Lett.* 2006;**429**(4-6):513-517. DOI:10.1016/j.cplett.2006.08.041
27. Kalantari M, Kazemeini M, Tabandeh F, Arpanaei A. Evaluation of biodiesel production using lipase immobilized on magnetic silica nanocomposite particles of various structures. *Biochem Eng J.* 2013;**79**:267-273. DOI: 10.1016/j.bej.2013.09.001

28. Hartley PA, Parfitt GD, Pollack LB. The role of the van der Waals force in the agglomeration of powders containing submicron particles. *Pow Tech*. 1985;**42**(1):35-46. DOI: 10.1016/0032-5910(85)80036-X
29. Banerjee SS, Chen DH. Magnetic nanoparticles grafted with cyclodextrin for hydrophobic drug delivery. *Chem Mater*. 2007;**19**(25):6345-6349. DOI: 10.1021/cm702278u
30. Woo E, Ponvel KM, Ahn IS, Lee C. Synthesis of magnetic/silica nanoparticles with a core of magnetic clusters and their application for the immobilization of His-tagged enzymes. *J Mater Chem*. 2010;**20**(8):1511-1515. DOI: 10.1039/B918682D
31. Lalatonne Y, Richardi J, Pileni MP. Van der Waals versus dipolar forces controlling mesoscopic organizations of magnetic nanocrystals. *Nat Mater*. 2004;**3**(2):121-125. PMID: 14730356
32. Xu XQ, Shen H, Xu JR, Xie MQ, Li XJ. The colloidal stability and core-shell structure of magnetite nanoparticles coated with alginate. *Appl Surf Sci*. 2006;**253**(4):2158-2164. DOI: 10.1016/j.apsusc.2006.04.015
33. Blaaderen AV, Geest JV, Vrij A. Monodispersed colloidal silica spheres from tetraalkoxysilanes particle formation and growth mechanism. *J Coll Inter Sci.* 1992;**154**(2):481-501. DOI: 10.1016/0021-9797(92)90163-G
34. Cheng Y, Tan R, Wang W, Guo Y, Cui P, Song W. Controllable synthesis and magnetic properties of Fe_3O_4 and Fe_3O_4@SiO_2 microspheres. *J Mater Sci*. 2010;**45**(19):5347-5352. DOI: 10.1007/s10853-010-4583-4
35. Lee J, Lee Y, Youn JK, Hyon BN, Yu T, Kim H, Lee SM, Koo YM, Kwak JH, Park HG, Chang HN, Hwang M, Park JG, Kim J, Hyeon T. Simple Synthesis of Functionalized Superparamagnetic Magnetite/Silica Core/Shell Nanoparticles and their Application as Magnetically Separable High-Performance Biocatalysts, Small. 2008;**4**(1):143-152. DOI: 10.1002/smll.200700456
36. Wonjin J, Kevin JF, Dong KY, Min JK. Fabrication of tunable silica-mineralized nanotubes using flagella as bio-templates. *Nanotech.* 2012;**23**(05):5601. DOI: 10.1088/0957-4484/23/5/055601
37. Qianjun H, Jianlin S, Feng C, Min Z, Lingxia Z. An anticancer drug delivery system based on surfactant-templated mesoporous silica nanoparticles. *Biomat*. 2010;**31**(12):3335-3346. DOI: 10.1016/j.biomaterials.2010.01.015
38. Huang S, Li C, Cheng Z, Fan Y, Yang P, Zhang C, Yang K, Lin J. Magnetic Fe_3O_4@mesoporous silica composites for drug delivery and bioadsorption. *J of Coll and Int Sci.* 2012;**376**:312-321. DOI: 10.1016/j.jcis.2012.02.031